MICHIGAN STATE UNIVERSITY

CYCLOTRON LABORATORY

NUCLEAR STRUCTURE OF EVEN-A CHROMIUM ISOTOPES IN THE BAND-MIXED PROJECTED HARTREE-FOCK MODEL

SURENDER SAINI and M.R. GUNYE

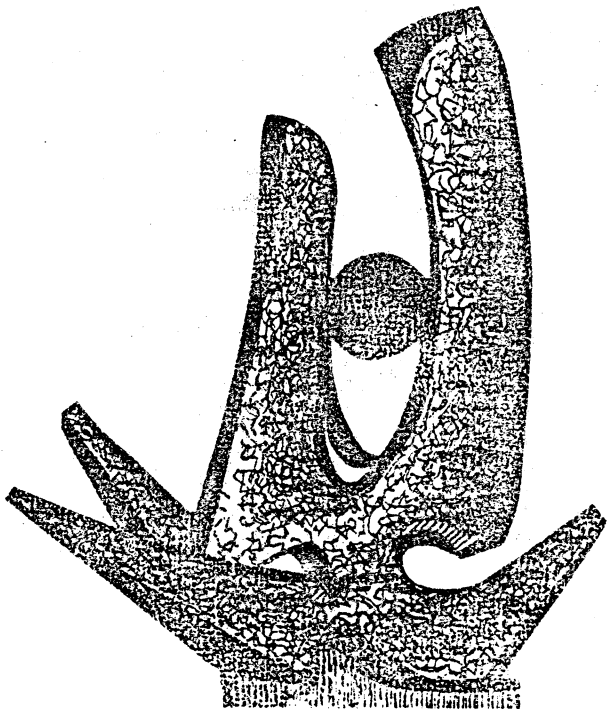

APRIL 1981

MSUCL-350

MSUCL-350
April 1981

Nuclear structure of even-A chromium isotopes in the band-mixed projected Hartree-Fock model

Surender Saini*

National Superconducting Cyclotron Laboratory
Michigan State University, East Lansing, MI 48824, U.S.A.

and

Nuclear Physics Division
Bhabha Atomic Research Center, Bombay 400085, India

M.R. Gunye

Theoretical Reactor Physics Section
Bhabha Atomic Research Center, Bombay 400085, India

ABSTRACT

Nuclear structure calculations for the states in even-A isotopes $^{48-54}$Cr are performed in the framework of projected Hartree-Fock model by employing a realistic nucleon-nucleon interaction. An inert ^{40}Ca core is assumed and all the valence nucleons are treated explicitly in the configuration space of the full fp shell. The energy levels, static electromagnetic moments and transition probabilities are evaluated from the band mixing calculations wherein a large number of energetically close intrinsic states of the nuclei are taken into account. These calculations yield a $K^{\pi} = 2^{+}$ and $K^{\pi} = 4^{+}$ highly deformed band for ^{50}Cr and ^{52}Cr respectively, when a neutron from the predominantly $(f_{7/2})^{n}$ lowest prolate intrinsic configuration is promoted to the higher unoccupied (fp) orbits. The results of the present calculations are in fairly good agreement with the available experimental data.

NUCLEAR STRUCTURE: Even-A chromium isotopes. Calculated spectra, static moments, transition strengths B(E2) and B(M1). Projected Hartree-Fock model with band mixing, $(fp)^{n}$ model space, modified Kuo-Brown interaction.

I. INTRODUCTION

The interest in studying the properties of the fp-shell nuclei is evident from the experimental and theoretical results published in literature in recent years. There is a significant increase in the amount of experimental information with the advent of heavy-ion induced reactions. This, in turn, has revived the interest in the theoretical studies of the structure of these nuclei. The early theoretical investigations on the structure of fp-shell nuclei were carried out in the framework of the spherical shell model[1] and the phenomenological deformed rotor-particle coupling (RPC) model.[2] The restricted shell model calculations[1] in a pure $(f_{7/2})^n$ configuration were able to account for a large amount of the then available experimental data on many fp-shell nuclei up to ^{56}Ni. The results of the empirical $(f_{7/2})^n$ shell model with various effective nucleon-nucleon (NN) interactions are published recently.[3] It is, however, quite obvious that the static and dynamic properties of many of the observed nuclear states cannot be described in terms of such restricted shell model calculations. The extension of the shell model configuration space to include the full fp-shell has led to a significant improvement[4,5] in correlating the observed properties of the nuclei with $A \leq 44$. Owing to the inherent complexities of the shell model calculations in a large configuration space of the full fp-shell, such calculations have not so far been reported for nuclei with $A > 44$. However, in view of the substantial pile-up of the experimental data, particularly on

the high-spin states populated in heavy-ion reactions, it is appropriate to make a systematic study of these nuclei employing a realistic NN interaction in a large configuration space of the complete fp-shell. The nuclear eigenstates are generated using the band mixed Hartree-Fock (HF) model which has been used[6,7] with success in Vanadium and Scanadium isotopes. The low-lying eigenstates of nuclei are assumed to be spanned by states of good angular momentum J, projected from several low-lying HF intrinsic states. The single and double nucleon excitations above the Fermi level are included in the non-orthogonal basis in which the nuclear Hamiltonian is then diagonalised to give the eigenstates of the nuclear system. This technique not only offers a massive truncation of the conventional shell model but also offers insight into the role of intrinsic shapes and their interaction. Moreover, in this scheme the Hamiltonian self consistently selects the most appropriate basis set. The collective behaviour occurring in the fp-shell nuclei with both protons and neutrons outside ^{40}Ca core can be understood by such realistic calculations. The chromium isotopes with four protons and many neutrons outside ^{40}Ca core can serve as good criteria for testing the efficacy of the realistic NN interaction used in the calculations.

We are concerned here with the nuclear structure of four even-A chromium isotopes $^{48-54}$Cr. In the calculations presented here, an inert ^{40}Ca core is assumed and all the four single particle states in the fp-shell are included in the active space. The calculations are performed in

the framework of HF projection formalism[8] employing the Kuo-Brown[9] effective NN interaction modified by McGrory.[5] The HF calculations with axially symmetric deformations show that there are many energetically close intrinsic states of the chromium nuclei under consideration here. This complication necessitates a band-mixing calculation to determine the admixture of various close-lying intrinsic states in the computed wavefunctions. The nuclear wavefunctions are, therefore, obtained from the good angular momentum states projected from the individual intrinsic bands by the band-mixing prescription.[10] The band-mixing HF projection formulation is outlined in Sec. II. The results of the calculations are discussed in Sec. III and the conclusions are presented in Sec. IV.

II. DESCRIPTION OF CALCULATIONS

The HF projection calculations for chromium isotopes under investigation are performed by employing the Kuo-Brown effective NN interaction as modified by McGrory.[5] All the valence nucleons outside an inert ^{40}Ca core are considered to be active in the configuration space of the full fp-shell. The single particle energies of the basis states $0f_{7/2}$, $1p_{3/2}$, $1p_{1/2}$ and $0f_{5/2}$ are taken to be 0.0, 2.1, 3.9 and 6.5 MeV respectively. The HF calculations are performed to obtain the intrinsic state Φ_K corresponding to the energy $E_K^{HF} = \langle\Phi_K|H|\Phi_K\rangle$ where H is the Hamiltonian of the nuclear system and K is the band quantum number. The HF calculations

in the chromium isotopes under consideration yield many energetically close intrinsic states. The good angular momentum states ψ_K^J projected[8] from different intrinsic states Φ_K may not be orthogonal. The nuclear wavefunction can then be expressed as

$$\Psi^J = \sum_K C_K^J \psi_K^J \qquad (1)$$

The nuclear Hamiltonian is diagonalized in the basis space of the good J states projected from the various intrinsic states. The band-mixing coefficients C_K^J and the energy ε^J of the nuclear state Ψ^J are obtained from the equation

$$\sum_{K'}\{\langle\psi_K^J|H|\psi_{K'}^J\rangle - \varepsilon^J\langle\psi_K^J|\psi_{K'}^J\rangle\} C_{K'}^J = 0 \qquad (2)$$

for each angular momentum state J. Thus, the energy ε^J of each nuclear state, is determined by solving the determinantal equation[10]

$$|\langle\psi_K^J|H|\psi_{K'}^J\rangle - \varepsilon^J\langle\psi_K^J|\psi_{K'}^J\rangle| = 0 \qquad (3)$$

The explicit expressions for the evaluation of the matrix elements $\langle\psi_K^J|H|\psi_{K'}^J\rangle$ and $\langle\psi_K^J|\psi_{K'}^J\rangle$ are given in Ref. 8. The static electromagnetic moments and transition probabilties can be computed by evaluating[11] the matrix elements of the relevant multipole operator between the initial and final nuclear states (eq. 1).

III. RESULTS AND DISCUSSION

The band-mixed wavefunctions[10] obtained from the self-consistent HF projection formalism are used in the nuclear

structure calculations of the four even-A chromium isotopes reported in this paper. The magnetic moment μ and the reduced transition probabilities B(M1) are calculated by employing the bare magnetic dipole operator corresponding to a free nucleon, whereas the electric quadrupole moment Q and the reduced transition probabilities B(E2) are evaluated by employing an effective quadrupole operator with effective charges assigned to the valence nucleons. The effective charges e_p = 1.33e for protons and e_n = 0.64e for neutrons adopted in the present calculations were obtained[12] by the least squares fit to the experimental B(E2) values in Ti, V, Cr and Fe isotopes in the mass region $44 \leq A \leq 54$.

The band quantum number K, the energy E_K^{HF} and the mass quadrupole moments $Q_K^{HF}(p)$ for protons and $Q_K^{HF}(n)$ for neutrons in the intrinsic states employed in the present band-mixing calculations in $^{48-54}Cr$ are shown in Table I. It should be noted that the prolate HF state is energetically the lowest state for all the four nuclei. The energy difference (in MeV) between the lowest oblate and the lowest prolate intrinsic states is 2.4, 2.0, 0.1 and 2.7 in ^{48}Cr, ^{50}Cr, ^{52}Cr and ^{54}Cr respectively. Thus the prolate-oblate energy difference is minimum for the nucleus ^{52}Cr corresponding to the closure of $f_{7/2}$ sub-shell for neutrons. The effect of the closure of the $f_{7/2}$ sub-shell for neutrons on the mass quadrupole moment $Q_K^{HF}(n)$ is quite conspicuous from Table I. The value (in fm^2) of $Q_K^{HF}(n)$ in the lowest prolate intrinsic state reduces drastically from 40.8 in ^{50}Cr to

9.9 in ^{52}Cr and then increases suddenly to 49.7 in ^{54}Cr. The change in $Q_K^{HF}(p)$ is, however, not so drastic as we go from ^{48}Cr to ^{54}Cr (see Table I).

It should be mentioned here that the energy of the next higher band in each of the nuclei is higher by about 1.0 MeV or more than that of the last band shown in Table I. It has been verified explicitly in one of the nuclei, ^{50}Cr, that the results of the band-mixing calculations are unaffected by including the next energetically higher band. The number of bands included in the present calculations is fairly optimum and the inclusion of more bands will lead to more complexities of calculations without significantly refining the results presented in this paper.

The recent experimental investigations[13] indicate the presence of a highly deformed excited band in some of the chromium isotopes. It is gratifying to note that the present HF calculations also yield a highly deformed prolate band in chromium isotopes corresponding to the excitation of a neutron from $f_{7/2}$ orbit to the higher orbitals. The band-mixing calculations show that this highly deformed band is characteristically different and does not mix with the other lower bands. Such an excited band has been indicated by an asterik in Table I.

The results of the nuclear structure calculations in $^{48-54}Cr$ by including the band-mixing between the intrinsic states displayed in Table I are discussed below.

^{48}Cr

A study of the self conjugate neutron deficient ^{48}Cr nucleus is of great interest because of its location in the middle of the $f_{7/2}$ shell. The shell model configuration of this nucleus is most complex in the $f_{7/2}$ shell, thereby providing a rigorous test for the various shell model techniques. Furthermore, this nucleus is expected to be highly deformed because of eight nucleons outside the closed ^{40}Ca core. Therefore, the low-lying spectrum of this nucleus is expected to show collective features such as deformed rotational bands.

Since this nucleus is some way off the line of stability, it is difficult to reach with either light or heavy ion reactions. Until recently, the information on the properties of low-lying levels in ^{48}Cr was rather scant. The earlier experimental studies[14-19] through the reactions $^{46}Ti(^{3}He,n)$ and $^{50}Cr(p,t)$ gave only rudimentary information on the level structure of ^{48}Cr. Kutschera et al.[20] measured the lifetimes of the first four yrast states populated via the $^{40}Ca(^{10}B,pn\gamma)^{48}Cr$ reaction. Haas et al.[21] employed the $^{34}S(^{16}O,2n\gamma)^{48}Cr$ reaction to study the low-lying yrast states in this nucleus. These authors[21] assigned $J^{\pi} = 6^{+}$ and $J^{\pi} = 8^{+}$ to the levels at 3533.7 and 4064.3 keV excitation energy. On the basis of these observations, they suggested the occurence of backbending in ^{48}Cr. More recent measurements of Ekström et al.[22] and Hansen et al.[23] through the reactions $^{36}Ar(^{14}N,pn\gamma)$ and $^{40}Ca(^{10}B,np\gamma)$, however, assign

a spin parity of 5^{-} and $6^{-}(7^{-})$ to the levels at 3533.7 and 4064.3 keV respectively. The 6^{+} and 8^{+} members of the yrast band have been identified[22,23] at 3447 and 5191 keV respectively. This interpretation[22,23] has removed any features suggestive of a backbending effect. Earlier theoretical calculations[19] for ^{48}Cr were carried out in the $(f_{7/2})^{8}$ shell model space. Recently Kutschera et al.[3] have performed shell-model calculations for ^{48}Cr in $(f_{7/2})^{8}$ configuration space employing five different sets of empirical two-body interactions. These restricted shell-model calculations[3,19] give a fair account of the observed energy spectrum. However, the B(E2) values for the γ-transitions between the low-lying yrast states computed[3] even with large effective charges $e_p = 1.9e$ and $e_n = 0.9e$ are substantially smaller than the corresponding experimental data.

The present calculations are carried out by employing the intrinsic states given in Table I. In addition to the lowest prolate and oblate HF solutions, three excited intrinsic states obtained by 1p-1h elementary excitations are included in the basis space. The energy spectrum of ^{48}Cr obtained from the present band-mixing calculations is displayed together with the experimental[14-23] energy spectrum in Fig. 1. The calculated excitation energies of the yrast states up to $J=8^{+}$ agree fairly well with the corresponding experimental energies. Ekström et al.[22] and Hansen et al.[23] observed a level at 7063 keV populated through $^{36}Ar(^{14}N,pn\gamma)$ and $^{40}Ca(^{10}B,np\gamma)$ reactions respectively. Hansen et al.[23] tentatively assigned J = (9,10) to this level on the basis

of their measurements. Our calculations predict the 10^+ member of the yrast band at an excitation energy of 6.52 MeV. We, therefore, suggest a J^π value of 10^+ for the observed level at 7063 keV. A number of 0^+ levels have been observed[16,18,19] in ^{48}Cr through $^{46}Ti(^3He,n)$ and $^{50}Cr(p,t)$ reactions. The observed[16,18,19] levels at 4280 keV and 8770 keV are very well reproduced by the present calculations. Our calculations predict the high spin members 12^+ and 14^+ of the yrast band to occur at 7.0 and 9.2 MeV excitation energy respectively. The shell model calculations[3] predict the corresponding energies to be 7.9 and 10.2 MeV respectively. The observed excited states with $J^\pi = 2^+$ and 4^+ are reproduced fairly well by the present calculations.

The present calculations yield the excitation energies (in MeV) 6.6, 4.6, 6.4, 8.0, 8.8 and 9.6 for the odd-J yrast states 3^+, 5^+, 7^+, 9^+, 11^+ and 13^+ respectively. These states have not been observed experimentally. The corresponding energies from the shell model calculations[3] are 5.3, 4.3, 5.9, 7.0, 8.6 and 11.5 MeV respectively. The results of the present calculations are thus in fair agreement with those of shell model calculations;[3] except for the energies of 3^+, 9^+ and 13^+ states. It is very much desirable to look for these states through heavy ion reactions.

It may be mentioned here that the lowest HF intrinsic state employed in the present calculations corresponds to a deformation $\beta = 0.28$, which agrees fairly well with the deformation of $\beta = 0.30$ obtained by Haas et al.[21] from the measured B(E2) values for $2^+ \rightarrow 0^+$ and $4^+ \rightarrow 2^+$ transitions.

The computed static electromagnetic moments for the low-lying states in ^{48}Cr are shown in Table II. It is unfortunate that no experimental data are available to test the calculated values. The magnetic moments obtained from the present calculations are in good agreement with those obtained from the shell model calculations[3] whereas the quadrupole moments differ drastically. It is, therefore, desirable to determine these static moments experimentally. The computed B(E2) and B(M1) values are presented in Table III. The experimental data is available only for a few γ-transitions. The calculated B(E2) values are in fair agreement with the available experimental values. The shell model calculations[3] predict highly retarded dipole transitions in contrast to the large B(M1) values predicted by our calculations. The B(E2) values predicted by the shell model calculations[3] even with large effective charges of $e_p = 1.9e$ and $e_n = 0.9e$ are substantially smaller than those obtained from the present calculations as can be seen from Table III.

^{50}Cr

Numerous experimental studies[24-35] have given rise to a wealth of information on the low-lying states in ^{50}Cr. The properties of the low-lying states up to $J^\pi = 6^+$ have been extensively studied through $(p,p'\gamma)$[24-28] (d,d'),[29] $(^3He,n)$,[33] $^{40}Ca(^{12}C,2p\gamma)$,[30] and $^{40}Ca(^{10}O,\alpha 2p\gamma)$[32] reactions. Kutschera et al.[31] identified the members of the yrast band up to $J^\pi = 12^+$ populated in the reactions $^{40}Ca(^{16}O,\alpha 2p\gamma)$,

$^{24}Mg(^{32}S,\alpha 2p\gamma)$, $^{40}Ca(^{14}N,3pn\gamma)$ and $^{40}Ca(^{12}C,2p\gamma)$. Recently Fahlander et al.[34] measured the g factor of 2^+ state in ^{50}Cr through the $^{50}Cr(^{16}O,^{16}O'\gamma)$ reaction. The nucleus ^{50}Cr is particularly interesting because its low energy structure shows[30] rather high collectivity. Measurements[35] of the static quadrupole moment of the 2^+ state suggests a large ground state deformation. However, the decrease of the B(E2) values of the ground state band with increasing spin indicates[30] a decrease of collectivity for the high spin states. It is, therefore, interesting to investigate the structure of ground state band; especially the collective nature of the high spin members of this band. The shell model calculations[1,3,36] in the pure $(f_{7/2})^n$ configuration space give a fair account of the experimental energy spectrum of ^{50}Cr. These simple shell model calculations, however, require very large effective charges to give any reasonalbe account of the reduced transition probabilities. The present band-mixing calculations are carried out by employing the intrinsic states given in Table I. The low-lying intrinsic states shown in Table I have dominantly a $(f_{7/2})^n$ character with small admixtures of the other higher lying (fp) shell orbits. The highly deformed one particle-one hole (lp-lh) intrinsic HF state (shown with an asterik in Table I) is obtained from the lowest prolate HF state, by promoting a neutron from the k = 5/2 deformed orbit of $f_{7/2}$ shell to the second k = 1/2 deformed orbit having large admixtures of $p_{3/2}$, $f_{5/2}$ and $p_{1/2}$ shell orbits. This is illustrated

in Fig. 2. The excited lp-lh intrinsic state of ^{50}Cr with K = 2 corresponds to the filling up of orbits at a larger deformation (Fig. 2(b)) as compared to the ground intrinsic state (Fig. 2(a)). It can be seen from Table I that the mass quadrupole moment $Q_K^{HF}(n)$ of the K = 2 lp-lh intrinsic state is substantially larger than that of the other low-lying HF states. It seems that the promoted neutron polarizes the valence $(f_{7/2})$ shell nucleons to a large extent giving rise to a large quadrupole moment for the K = 2 intrinsic state. The deformed lp-lh instrinsic state employed in our calculation is, therefore, much more complex than the configurations of the type $(0f_{7/2})^{n-1}$ $(1p_{3/2},1p_{1/2},0f_{5/2})^1$ employed in the conventional shell model calculations.

The energy spectrum obtained from the present band-mixing calculations is displayed in Fig. 3 along with the experimental energy levels. It can be seen from FIg. 3 that the excitation energies of the yrast states up to $J^\pi = 11^+$ are very well reporduced by our calculations. The yrast and yrare states with $J^\pi = 12^+$ are predicted at excitation energies of 6.5 and 7.8 MeV respectively. The predicted energy of the 12^+ yrare state agrees well with that of the observed 12^+ state. It will be interesting to see whether there exists a 12^+ state at 6.5 MeV excitation as predicted by the present calculations. The excitation energies of the yrast states with $J^\pi = 3^+$ and 5^+ are reproduced reasonably well by the present calcualtions. The present calculations predict the yrast 7^+ and 9^+ states at an excitation energy

of 5.2 and 6.6 MeV respectively. These two yrast states have not been observed so far experimentally. The excitation energies of the 7^+ and 9^+ states are in good agreement with those obtained from the shell-model calculations.[3] The 14^+ and 16^+ members of the yrast band are predicted to occur at excitation energies of 8.7 and 10.0 MeV respectively by the present calculations. The present band mixing calculations also give a good account of the observed excitated states. The 0^+ states at 3698 keV and 5760 keV, 2^+ states at 2925 keV and 6450 keV, and 4^+ states at 3324 keV and 3938 keV, observed[16,27,28,33] in (^{3}He,n), (p,t) and (p,p'γ) experiments, are reproduced fairly well as can be seen from Fig. 3.

As discussed earlier, the present calcualtions indicate the presence of a highly deformed $K = 2^+$ band which does not mix with any of the other low-lying bands. The energy spectrum projected from this band is also shown in Fig. 3. The experimentally observed 2^+, 3^+ and 4^+ at 3.16, 3.59 and 3.61 MeV excitation energy respectively can be identified as the members of this $K = 2^+$ band. The projected energy spectrum from this band (Fig. 3) is shifted downwards by 1.4 MeV so as to fit the energy of the band head. The excitation energies (in MeV) of the high spin members of this collective band, as predicted by the present work, are: 5^+ (4.45) 6^+ (5.09), 7^+ (5.79), 8^+ (6.62), 9^+ (7.49), 10^+ (8.45) 11^+ (9.00) and 12^+ (9.50). Such highly deformed collective bands have been observed[13,37-40] in many N = 27, 28 and 29 nuclei. It will be, therefore, very interesting to identify

the high spin members of the K = 2 collective band through heavy-ion reactions. The heavy-ion reactions have a high selectivity in populating a particular type of states.

The calculated static electromagnetic moments for the yrast states 2^+, 4^+ and 6^+ are given in Table II. The experimental values are available[34,35] only for the 2^+ yrast state. The agreement between the calculated and the experimental values is fair as can be seen from Table II. The magnetic moments obtained from the $(f_{7/2})^n$ shell model calculations[3] are in fair agreement with those obtained from the present calculations. However, the quadrupole moments obtained from the shell model calculations[3] even with large effective charges (e_p = 1.9e and e_n = 0.9e) are substantially smaller than those obtained in our calculations. The calculated reduced transition probabilities are presented in Table IV. The calculated values are in fair agreement with the available experimental data except for the $2_1^+ \rightarrow 2^+$ transition. The calculated B(M1) values for the $11^+ \rightarrow 10^+$ and $12^+ \rightarrow 11^+$ γ transitions are in fair agreement with the experimental values. The calculated M1 transition strengths for the $2_1^+ \rightarrow 2^+$ and $4_1^+ \rightarrow 4^+$ transitions are, however, smaller by a factor of two to three than the corresponding experimental values. It should be pointed here that the lowest prolate and oblate HF states in the present calculations correspond to a deformation of $\beta = 0.23$ and 0.14 respectively. The deformation β for the 2^+, 4^+, 6^+, 8^+ and 10^+ states, derived from the calculated quadrupole moments and B(E2)

values, is 0.23, 0.21, 0.15, 0.16, 0.15 respectively; which clearly shows that the collectivity decreases as we go to high spin states. The oblate intrinsic state contributes significantly to the high spin states.

^{52}Cr

In recent years, the low-lying states of the N = 28 isotones have been the object of numerous experimental and theoretical investigations. Assuming that only pure $(0f_{7/2})^n$ configurations are responsible for the low energy states, one expects to observe excited states up to $J^\pi = 8^+$ in ^{52}Cr. All these states have indeed been observed in ^{52}Cr through a variety of nuclear reactions (Refs. 13,16,32,33,42-64). Of greater interest, however, are the high spin states which are expected to arise from core excitations. Some of the high spin states in ^{52}Cr have been studied recently by Berinde et al.[61] using the ^{50}Ti(α,2nγ) reaction and by Poletti et al.[62] using the ^{51}V(^{7}Li,α2nγ) reaction. Styczen et al.[13] recently studied the states up to $J^\pi = 11^+$ in ^{52}Cr populated through ^{50}Ti(α,2nγ) reaction. The experimental studies of Styczen et al.[13] indicate the presence of a $K = 4^+$ highly deformed excited band in ^{52}Cr.

The nuclear structure of the low-lying levels of N = 28 isotones has been investigated (Refs. 1,3,13,32,56,65-78) in the framework of shell model with varying degrees of sophistication concerning the model space and the consideration of some supplementary degrees of freedom like vibrations and rotations. The earlier shell model calculations[1,65,66]

for ^{52}Cr were performed by assuming a pure $(f_{7/2})^n$ configuration for the protons outside the ^{48}Ca core. The description in terms of simple $(f_{7/2})^n$ configurations was rather satisfactory for many of the observed low-lying levels. These restricted $(f_{7/2})^n$ shell model calculations[1,3,65,66], however, do not account for the observed density of levels at excitation energies ≥ 2 MeV and do not describe some features of the nuclear transfer reaction data. Moreover, M1 transitions are forbidden between the $(f_{7/2})^n$ configuration states as are the E2 transitions between the states of the same seniority. These forbidden transitions, however, are found to occur between the observed levels, thereby indicating the presence of configuration admixtures. Furthermore, the positive-parity levels with spins exceeding the maximum angular momenta allowed by the $(f_{7/2})^n$ representation have been observed[13,61] recently in ^{52}Cr. Auerbach,[67] and Lips and McEllistrem[68] included single proton excitations from $f_{7/2}$ shell to $p_{3/2}$ and $f_{5/2}$ orbitals. These shell model calculations in the expanded configuration space showed a considerable improvement over the $(f_{7/2})^4$ model calculations and provided a good representation of the low-lying levels with $J^\pi \leq 8^+$. In the follow up study of configuration mixing effects, Rustgi et al.[69] carried out the shell model calculations in the $(fp)^4$ configuration space employing the renormalized Kuo-Brown matrix elements for the two-body effective interaction. The mixed configuration shell-model calculations[67-69] mentioned above employ wavefunctions which do not have good isospin

structure. The calculations of Osnes,[71] Roy et al.,[70] Pellegrini et al.[52] and Chuu et al.[72] is an improvement over the earlier calculations since the wavefunctions with good isospin structure are used by taking the corresponding neutron excitations into account. Though all the calculations mentioned above give a fairly good description of low-lying states with $J^{\pi} \leq 8^{+}$, none of these calculations predict high spin states with $J^{\pi} \geq 8^{+}$. Recent shell model calculations of Haas et al.,[73] Yokoyama et al.[74] and Styczen et al.[13] show that the high spin states with $J \geq 8^{+}$ can only be generated by a single neutron excitation to the higher fp orbitals. Most of these shell model calculations, however, use empirical NN interactions. Sharma[76] has investigated the structure of low-lying levels in ^{52}Cr in the framework of Hartree-Fock Bogoliubov formalism using realistic NN effective interaction. The predicted 2^{+} and 4^{+} yrast states are very much lowered in energy as compared to the corresponding experimental levels. Moreover these calculations[76] do not investigate the high spin states and the transition probabilities. Recently Müther et al.[77] have investigated the structure of high spin yrast states in a microscope approach allowing a coupling of rotations, vibrations and quasiparticle excitations. Their calculated yrast states with $J^{\pi} > 4^{+}$ are too high in energy as compared to the corresponding observed levels. These authors[77] do not calculate B(E2), B(M1) and the static moments. Very recently Ahalpara[78] has investigated the nuclear structure of the low-lying

levels in ^{52}Cr in the framework of HF projection formalism employing only the lowest intrinsic state and an excited one particle-one hole state. These calculations[78] do not predict many excited levels belonging to the ground state band. Moreover, the electromagnetic properties are very sensitive to the mixing between different intrinsic states. It is, therefore, very much desirable to do a band-mixing calculation employing a realistic NN interaction in the full fp shell.

The present band-mixing calculations are performed by employing the intrinsic states listed in Table I. In addition to the lowest (K = 0) prolate and oblate HF solutions, a number of excited intrinsic states obtained by lp-lh elementary excitations were included in the calculations. The excited lp-lh intrinsic states (shown without an asterik in Table I) obtained by proton excitations have the same basic character as the ground K = 0 HF intrinsic states. These intrinsic states are predominantly made of spherical $(f_{7/2})^{n}$ configurations with very little admixtures of other higher lying fp shell orbits. On the average the intensity of the $(f_{7/2})^{n}$ component in these intrinsic states is 96%. On the other hand, the excited lp-lh intrinsic state obtained by promoting a neutron from the k = 7/2 deformed orbit of $f_{7/2}$ shell to the second k = 1/2 deformed orbit contains large admixtures of higher fp shell orbits with only 40% strength of $(f_{7/2})^{n}$ configurations. It can be seen from Table I that the mass quadrupole moment $Q_{K}^{HF}(n)$ of this K = 4 intrinsic state is 4 times larger than that of the other

low-lying intrinsic states. We find that the good J states projected from this intrinsic state do not mix with the states projected from the other low-lying intrinsic states.

The energy levels of ^{52}Cr obtained from the present band-mixing calculations are compared with the observed spectrum in Fig. 4. The left-hand part of the spectrum exhibits levels belonging to the ground state band which has a predominant $(f_{7/2})^n$ component, where as the right-hand part of the spectrum shows the strongly deformed collective states belonging to the collective K = 4 band. It can be seen from Fig. 4 that the excitation energies of the yrast sequence of states with $J^\pi = 2^+, 4^+, 5^+ 6^+$ and 8^+ are very well reproduced by our calculations. The first excited 2^+ and 4^+ states observed (Refs. 13, 32, 33, 52, 54, 61 62) at 2965 and 2768 keV respectively, are also predicted correctly by the present calculations. Bohne et al.[33] observed a 2^+ state at 8710 keV populated in the $^{50}Ti(^3He,n)^{52}Cr$ reaction. This 2^+ state is very well reproduced by our calculations. A number of 0^+ states have been observed[16,33,51,52] in ^{52}Cr through $(^3He,n)$ and (t,p) reactions. The observed[33,52] 0^+ levels at 7450 and 9580 keV are fairly well reproduced by the present calculations.

It should be mentioned here that the earlier microscopic calculations of Sharma,[76] Müther et al.,[77] and Ahalpara;[78] do not investigate any of the yrare states belonging to the ground state band. The present calculations predict a few excited states which do not have any experimental

counterparts. The excitation energies (in MeV) of these states are $2^+(9.92)$, $4^+(8.50,10.38)$, $6^+(7.98, 10.00)$ and $8^+(9.86, 11.50)$. Styczen et al.[13] in their recent ^{50}Ti $(\alpha,2n\gamma)$ studies indicate the presence of a level at 6365 keV, which decays by a weak γ transition to a 8^+ level at 4750 keV. These authors[13] tentatively assign a spin of (>8) to this level at 6365 keV. This level, however, was not observed in the earlier $^{50}Ti(\alpha,2n\gamma)$ and $^{51}V(^7Li,\alpha 2n\gamma)$ studies of Berinde et al.[61] and Poletti et al.[62] respectively. Our calculations do not predict any high spin state with $J \geq 8$ around 6.4 MeV excitation energy. The present calculations, however, indicate the presence of 9^+ state at 9.76 MeV. This particular state arises only from the 1p-1h intrinsic states obtained by the proton excitations and has appreciable admixtures of the $p_{3/2}$, $f_{5/2}$ and $p_{1/2}$ orbitals. The lowest prolate and oblate intrinsic states with a dominant $(f_{7/2})^n$ component do not give states with $J > 8^+$.

As pointed out earlier in the discussion, the recent experimental measurements[13,61] indicate an evidence for a sequence of states built on an excited $K = 4^+$ collective band. The energy spectrum projected from the highly deformed $K = 4^+$ band is compared with the observed[13,61] collective band of states in Fig. 4. It should be noted that the calculated energy spectrum is shifted downwards by 2.3 MeV so as to fit the energy of the $J^\pi = 4^+$ band head and facilitate a comparison with the experimental energy spectrum. The excitation energies of the collective band of states relative

to the band head $J^\pi = 4^+$, are fairly well described by the present calculations.

The calculated static electromagnetic moments for the low-lying positive parity yrast states are compared with the available experimental[35] data and the shell model calculations[3,35] in Table II. The measured[35] quadrupole moment for the 2^+ yrast state has a large uncertainty. The present calculations predict a small quadrupole moment for the 2^+ yrast state as compared to the corresponding experimental value. The pure $(f_{7/2})^n$ shell model calculations[3] predict vanishing quadrupole moments for all the low-lying yrast states in ^{52}Cr. The quadrupole moment of the 2^+ yrast state predicted by the configuration-mixing shell model calculations of Towsley et al.[35] is in fairly good agreement with our result. The experimental data on the magnetic moments are not available for comparison. The magnetic moments predicted by the present calculations are in good agreement with the results of pure $(f_{7/2})^n$ shell model calculations.[3] The earlier microscopic calculations of Sharma,[76] Müther et al.,[77] and Ahalpara[78] do not report any results on the static moments of the low-lying yrast states in ^{52}Cr.

The B(M1) and B(E2) values for the γ transitions between the members of the ground state band are presented in Table V. The observed E2 transition strengths for most of the γ transitions are fairly well reproduced by the present calculations. The present calculations, however, do not reproduce the experimental B(E2) values for the $2^+ \to 0^+$, $5^+ \to 4^+$, $8^+ \to 6^+$,

$4_1^+ \to 2^+$ and $6^+ \to 4_1^+$ transitions. Our calculated value for the $2^+ \to 0^+$ transition is smaller than the corresponding experimental value by a factor of 2. On the other hand $(f_{7/2})^n$ shell model calcualtions reproduces fairly well the observed B(E2) value for this transition; indicating thereby that the 2^+ state has a relatively pure $(f_{7/2})^n$ structure. The excited intrinsic states employed in the present calculations, however, contain sizable admixtures of the higher (fp) shell orbits. It should be pointed out that the restricted $(f_{7/2})^n$ shell model calculations employ very large effective charges. The lowest prolate HF intrinsic state gives a B(E2) value of 96 e^2fm^4 for $2^+ \to 0^+$ transition, which is in better agreement with the observed value. The present calculations predict a large B(E2) value for the $5^+ \to 4^+$ transition, whereas the pure $(f_{7/2})^n$ shell model calculations predict vanishing E2 transition strength for this transition. Experimentlaly a weak $5^+ \to 4^+$ transition is observed[13,55] and the measurements of Sprague et al.[55] put an upper limit of 30 e^2fm^4 on the B(E2) value for this transition. The observed B(E2) values for the $8^+ \to 6^+$, $4_1^+ \to 2^+$ and $4_1^+ \to 4^+$ transitions are quite uncertain due to large errors. Our calculated B(E2) value for the $8^+ \to 6^+$ transition is substantially smaller than the corresponding measured value and the one predicted by the $(f_{7/2})^n$ shell model calculations. According to the seniority selection rule, the $2_1^+ \to 0^+$, $2_1^+ \to 4^+$, $4_1^+ \to 2^+$, and $6^+ \to 4_1^+$ E2 transitions are strictly forbidden in the $(f_{7/2})^n$ model. Our calculations predict finite, though small, B(E2) values for these

transitions. The present calculations, however, do not reproduce the measured B(E2) values for these transitons. It should be mentioned here that the recent configuration mixing shell model calcuations of Styczen et al.[13] predict B(E2) values of 10.4 and 11.9 e^2fm^4 for $4_1^+ \rightarrow 2^+$ and $6^+ \rightarrow 4_1^+$ transitions respectively, which are very close to the predictions of the present calculations.

The observed M1 transitions between the positive parity states in the ground state band are highly retarded and have large uncertainties. The M1 transitions are strictly forbidden in the pure $(f_{7/2})^n$ model. The B(M1) values predicted by the present calculations for the $5^+ \rightarrow 4^+$, $5^+ \rightarrow 6^+$, and $4_1^+ \rightarrow 4^+$ γ transitions are in very good agreement with the recent measurements of Styczen et al.[13] It should be mentioned here that the shell model calculations[13] in the $(f_{7/2})^n + (f_{7/2})^{n-1}(p_{3/2}f_{5/2}p_{1/2})^1$ model space give very small B(M1) values for these transitions. Our calculated M1 strength for the $2_1^+ \rightarrow 2^+$ is slightly larger than the corresponding experimental value. It can be seen from Table V that the B(M1) value for this transition, obtained from configuration mixing shell model calculations, agrees fairly well with our calculated value.

The B(M1) and B(E2) values for the intraband transitions between the members of the excited $K = 4^+$ collective band are presented in Table VI. It can be seen from Table VI that these transitions are quite enhanced as compared to those for the "ground state band". It should be mentioned here that all the collective band of states arise from the

highly deformed 1p-1h intrinsic state (obtained by the promotion of a neutron to the higher deformed orbital) which has a dominant $p_{3/2}$ component with appreciable admixtures of $f_{5/2}$ and $p_{1/2}$ shells. As a consequence, these states are expected to decay preferentially by M1 mode. This expectation, to a good extent, is in agreement with the experimental measurements.[13] The measured B(E2) and B(M1) values are quite uncertain due to large errors. Within the experimental errors, the measured B(E2) values are very well reproduced by the present calculations. The configuration mixing shell model calculations,[13] on the other hand, give substantially small B(E2) values for most of the transitions. It can be seen from Table VI that the strength of the pure E2 transitions is roughly the same except for the $6^+ \rightarrow 4^+$ and $7^+ \rightarrow 5^+$ transitions. Within the experimental uncertainties, the observed B(M1) values for the $5^+ \rightarrow 4^+$ and $6^+ \rightarrow 5^+$ transitions are fairly well reproduced by the present calculations, whereas the shell model calculations of Styczen et al.[13] predict a very large B(M1) value for the $6^+ \rightarrow 5^+$ transition. Our calculated M1 strengths for the other transitions are an order of magnitude larger than the corresponding measured values. Because of entirely different deformations in the 'ground state band' and the 'excited $K = 4^+$ collective band', the states belonging to these two bands do not couple. Therefore, the interband transitions between the members of the 'collective band' and those belonging to the 'ground state band' (with dominant $(f_{7/2})^n$ spherical character), are expected to be extremely hindered.

^{54}Cr

The level structure of ^{54}Cr has been studied by β^- decay[79] of ^{54}V, coulomb excitation (Refs. 35, 42, 80, 81); and through such nuclear reactions as (p,p'),[24,28] (n,γ),[83,84] (d,d),[85-87] (d,p) (Refs. 24, 82, 85-88) and (t,p).[51] Recently Nathen et al.[89] have investigated the high spin yrast states up to $J^\pi = 10^+$ populated through fusion-evaporation reactions induced by ^9Be, ^{11}B and ^{13}C heavy-ion beams. The low-lying levels of ^{54}Cr have been investigated in detail by Nathen et al.[90] recently through a study of the β-delayed γ-ray activity from $^{48}Ca(^9Be,p2n)^{54}V(\beta^-)^{54}Cr$. The first nuclear structure calculations for this nucleus were performed by Vervier[91] by restricting the valence particles to the $\pi(0f_{7/2})^4\nu(1p_{3/2})^2$ configuration space outside the ^{48}Ca core. The neutron-proton (np) interaction matrix elements were derived from a modified δ interaction in these calculations. These shell model calculations[91] were able to give a reasonable account of many of the low-lying levels in ^{54}Cr. McGrory[92] improved the previous shell model calculations[91] by extending the model space. In these calculations,[92] the protons and neutrons outside the ^{48}Ca core were restricted to the configuration space $\pi(0f_{7/2})^4x\nu(1p_{3/2},1p_{1/2},0f_{5/2})^2$ and the np interaction was taken to be a modified δ interaction introduced by Vervier.[91] These calculations,[92] though, gave a fairly good description of low-lying levels up to 3 MeV excitation; indicate that the configuration mixing effects due to proton excitations from $f_{7/2}$ to higher fp

orbitals become significant above 3 MeV excitation energy. The predicted[92] spectroscopic strengths for the (p,d) reaction also indicate that the neutron core-excited states play a significant role even in low-lying levels. The shell model calculations of VerVier,[91] and McGrory,[92] however, do not investigate the yrast states with $J^\pi > 4^+$. Moreover, the transition rates and the static moments are not investigated by these authors.[91,92] Horie and Ogawa[93] carried out shell-model calculations in the same configuration space as that of McGrory by employing an np interaction determined by a least square fit to the observed spectra of N = 29 nuclei. They also investigated the effect of neutron-proton correlations in N = 29 and N = 30 nuclei. These calculations[93] indicate that strong correlations between protons and neutrons breakdown the pairing scheme and lower the first 2^+ levels in doubly even nuclei. The calculations of Horie and Ogawa[93] give a fairly good account of the even J yrast states up to 10^+. These calculations[93] also indicate that the collective rotational like behaviour of these states arises due to strong np correlations. These authors,[93] however, use very large effective charges to give a reasonable account of the quadrupole moment and the B(E2) value for the first 2^+ state. The electromagnetic properties of the higher levels are not investigated in this work.[93] It has been noted by Bhatt, Parikh, and McGrory[94] and recently by Ogawa[95] that because of the quadrupole-quadrupole (Q.Q) dominance of the effective np interaction, the low-lying states of ^{54}Cr can be described in terms of the coupling

of a small number of low-lying collective states of the proton and neutron groups. This method[94,95] offers a considerable truncation of the configuration space, since only neutron and proton configurations with large diagonal and off-diagonal matrix elements of the quadrupole operator are sufficient to be included. These calculations[94,95] give a fairly good account of the low-lying levels in ^{54}Cr. The high spin yrast states are, however, not investigated by these authors.[94,95] Recently Nathan et al.[89] have investigated the high spin yrast states in their shell model calculations. These calculations[89] give a fairly good account of the even J yrast states. These authors,[89] however, employ very large effective charges to calculate B(E2) values. It should be mentined here that all the shell model calculations mentioned above, employ empirical NN interactions. As pointed out by Horie and Ogawa,[93] excitations of a nucleon from $f_{7/2}$ shell are enhanced by the strong correlations between two nucleons in the upper fp shells. In the case of ^{54}Cr, however, where the two nucleons exist outside the ^{48}Ca core, the excitation of a neutron from the $f_{7/2}$ shell might contribute less than in the N = 28 and 29 nuclei. However, the proton excitations from the $f_{7/2}$ shell to the upper shells might be important for some of the states in ^{54}Cr. It is, therefore, appropriate to investigate the nuclear structure of the low-lying levels of ^{54}Cr by employing more realistic NN interactions in the configuration space of the full (fp) shell.

In addition to the lowest prolate and oblate HF states, a number of excited intrinsic states obtained from the lowest HF states by 1p-1h and 2p-2h elementary excitations are included in the present calculations. A preleminary version of these calculations has been reported elsewhere.[96] The intrinsic states employed in the present band-mixing calculations are shown in Table I. The energy spectrum obtained from the present band-mixing calculations is compared with the experimental spectrum in Fig. 5. The even-J yrast states consists of a $\Delta J=2$ sequence extending from the 0^+ ground state to the 10^+ level at 6720 keV. The excitation energies of the sequence of these even-J yrast states are fairly well reproduced by the present calculations (Fig. 5) and are suggestive of a rotational like behaviour. The enhancement of the observed and calculated E2 transition strengths (Table VII) lend additional support to this picture. The present calculations predict the 12^+ member of the even-J yrast band of states to occur at 8.33 MeV, wehreas the shell model calculations of Horie and Ogawa[93] predict this state to occur at about 9.5 MeV.

The observed excitation energies of the first excited 2^+, 4^+, and 6^+ states are reproduced fairly well by our calculations. The present calculations, however, predict the excitations energies of the 7^+ and 9^+ yrast states higher, by about 1.6 and 2.5 MeV respectively, than the corresponding experimental energies. It is interesting to note that the recent shell model calculations of Nathan et al.[89] also

predict the excitation energies of the 7^+ and 9^+ yrast states higher, by about 1.2 and 1.6 MeV respectively, than the corresponding experimental energies. The yrast states 3^+, 5^+, and 11^+ have not been observed so far experimentally. Our calculations predict the yrast states 3^+, 5^+, and 11^+ to occur at excitation energies of 4.6, 3.9 and 9.9 MeV respectively. Our predicted energy for the 5^+ yrast state is very close to the shell model results of Horie and Ogawa.[93] These calculations,[93] however, predict the 3^+ yrast state about 1.4 MeV lower in energy than our prediction. The present calculations predict three 2^+ excited states at 5.36, 5.99 and 8.44 MeV, and the first two excitation energies agree very well with the experimentally observed levels at 5.49 and 6.15 MeV. The levels at 5.49 and 6.15 MeV were assigned a spin-parity of $(1,2)^+$ in the (d,d) and (d,p) measurements (Refs. 85-88). On the basis of the present calculations, we therefore suggest a spin parity of 2^+ for both of these levels. The present work predict the excited first 0^+ level at 3.77 MeV, which is about 900 keV too high compared with the corresponding observed (Refs. 24, 51, 82-88) 0^+ level at 2.83 MeV. Our calculated energy of the 0^+ level, however, is very close to the excited second 0^+ level at 4.01 MeV observed in (p,p'), (d,p) and (t,p) work (Refs. 24, 51, 85-88). It is very tempting to point out that our calculated 0^+ level at 3.77 MeV may correspond to the observed 0^+ level at 4.01 MeV.

The present calculations also predict a few excited states which have not been experimentally identified so far. The excitation energies in (MeV) of these states are

$0^+(6.36, 8.61)$, $2^+(8.44)$, $3^+(6.44)$, $4^+(5.79, 8.50)$, $5^+(5.53, 6.72)$, $6^+(6.50, 6.88)$, $7^+(7.20)$, and $8^+(6.12, 7.99)$.

The calculated static electromagnetic moments for the low-lying positive parity yrast states are shown in Table II. The experimental data[34,35] on the static moments is available only for the 2^+ yrast state. The results of our calculations are in fairly good agreement with the experimental values. The shell model calculations[35] in the $(f_{7/2})^{12}(p_{3/2})^2$ + $(f_{7/2})^{11}(p_{3/2}f_{5/2})^3$ configuration space give vanishingly small value for the quadrupole moment of the 2^+ yrast state. On the other hand, the shell model calculations of Horie and Ogawa,[93] by assuming configurations of the type $\pi(f_{7/2})^4$ $\nu(p_{3/2},p_{1/2},f_{5/2})^2$ outside the ^{48}Ca core, give results similar to our calculations. These shell model calculations,[93] however, use very large effective charges. The B(E2) and B(M1) values for the γ transitions between the low-lying positive parity states in ^{54}Cr are presented in Table VII. The experimental data on B(M1) values are not available for comparison. The results of our calculations are in fairly good agreement with the available experimental data on B(E2) values. The shell model results of Nathan et al,[89] for the even-J yrast states, are similar to our calculations. These shell model calculations,[89] however, employ very large effective charges to reproduce the observed B(E2) values. The shell model results for the transition strengths of the other excited states are not available for comparison.

IV. CONCLUSIONS

The properties of the nuclear levels in even-A chromium isotopes are investigated in the framework of Hartree-Fock formalism by employing the effective NN interaction.[5,9] All the nucleons outside the inert ^{40}Ca core are explicitly treated in the configuration space of the complete fp shell. The energy levels and the electromagnetic properties of the low-lying levels in $^{48-54}Cr$ are calculated by band mixed wave functions. The present calculations strongly suggest that the low-lying excited bands in ^{50}Cr and ^{52}Cr (with N = 26 and 28) are likely to be highly deformed collective states in contrast to the 'ground band of states' which have a predominant $(f_{7/2})^n$ character. These excited collective bands arise as a result of the promotion of a neutron from the highest occupied k = 5/2 or 7/2 orbit to the next k = 1/2 deformed orbit, having large admixtures of the j = $p_{3/2}$, $p_{1/2}$ and $f_{5/2}$ states. This brings about a large change in quadrupole moment and hence resulting in core polarization. This, however, would not be possible if k = 1/2 deformed orbit is completely full in the ground state configuration. Therefore, excited collective bands are not expected to occur in nuclei with $N \geq 30$.

The present calculations give a fairly good description of the observed nuclear levels, including those with high angular momentum. The excitation energies of the collective band of states relative to the band head $J^\pi = 2^+$ in ^{50}Cr and $J^\pi = 4^+$ in ^{52}Cr are fairly well reproduced by the present

calculations. Our calculations, however, fail to reproduce the excitation energy of the band head state of the $K = 2^+$ and $K = 4^+$ 1p-1h collective band. This may be due to the limitations of the effective NN interaction employed in the present calculations. There are indications[78,97] that the modified Kuo-Brown[5,9] interaction does not give good description for the states which have dominant $p_{3/2}$ component with significant admixtures of $p_{1/2}$ and $f_{5/2}$ orbitals. The excitation energies of the high spin yrast states and many excited states, not observed so far experimentally, are predicted. The calculatons also predict the high spin members (up to $J^\pi = 12^+$) of the $K = 2^+$ collective band in ^{50}Cr; and 12^+ member of the $K = 4^+$ collective band in ^{52}Cr. The static electromagnetic moments for the low-lying yrast states agree fairly well with the experimental values wherever available. The shell model calculations predict vanishing quadrupole moments for the 2^+, 4^+ and 6^+ yrast states in ^{48}Cr, whereas the present calculations predict large quadrupole moments for these states. The calculated B(E2) values are in good agreement with the experimental data for most of the γ transitions. The calculated B(M1) values, though agree fairly well in many cases, deviate substantially from the experimental values in a few cases. The transition strengths for a large number of transitions between the excited states have been calculated. It will be interesting to look for the predicted high spin yrast states in $^{48-54}Cr$ and the high spin members of the $K = 2^+$ collective band in ^{50}Cr through heavy-ion reactions, and to measure the

quadrupole moment of the 2^+ yrast state in ^{48}Cr, and the transitions strengths of the high spin states in these nuclei.

REFERENCES

* On leave of absence from Bhabha Atomic Research Center, Bombay 400085, India.

1. J.D. McCullen, B.F. Bayman and L. Zamick, Phys. Rev. 134, B515 (1964).
2. F.B. Malik and W. Scholz, Phys. Rev. 150, 919 (1966); W. Scholz and F.B. Malik, ibid 153, 1071 (1967).
3. W. Kutschera, B.A. Brown and K. Ogawa, Rev. Del. Nuovo Cim. 1, no. 12 (1978).
4. J.B. McGrory, B.H. Wildenthal and E.C. Halbert, Phys. Rev. C 2, 186 (1970).
5. J.B. McGrory, Phys. Rev. C 8, 693 (1973).
6. S. Saini and M.R. Gunye, J. Phys. G 4, 219 (1978); Phys. Rev. C 22, 2575 (1980).
7. S. Saini and M.R. Gunye, Phys. Rev. C 18, 2749 (1978); J. Phys. G 4, 1725 (1978); in Proceedings of the International Conference on Nuclear Structure, Tokyo, 1977 (International Academic Printing Co. Ltd., Tokyo, 1977), p. 240.
8. C.S. Warke and M.R. Gunye, Phys. Rev. 155, 1084 (1967); M.R. Gunye, Phys. Lett. 27B, 136 (1968).
9. T.T.S. Kuo and G.E. Brown, Nucl. Phys. A114 241 (1968).
10. S. Saini, Ph.D. thesis, University of Bombay, 1979 (unpublished).
11. M.R. Gunye and C.S. Warke, Phys. Rev. 159, 885 (1967).
12. A.K. Dhar and K.H. Bhatt, Phys. Rev. C16, 792 (1977).
13. J. Styczen et al., Nucl. Phys. A327, 295 (1979).

14. R.G. Miller and R.W. Kavanagh, Nucl. Phys. A94, 261 (1967).

15. O.D. Brill, A.D. Vongai, V.S. Romanov and A.R. Faiziev, Sov. J. Nucl. Phys. 12, 138 (1971).

16. D. Evers, W. Assmann, K. Rudolph, S.J. Skorka and P. Sperr, Nucl. Phys. A230 1, 109 (1974).

17. J.F. Bruandet, N. Longequeue, J.P. Longequeue and B. Vignon, Phys. Lett. 37B, 58 (1971).

18. W.E. Dorenbusch, J.B. Ball, R.L. Auble, J. Rapaport and T.A. Belote, Phys. Lett. 37B, 173 (1971).

19. J.R. Shepard, R. Graetzer and J.J. Kraushaar, Nucl. Phys. A197, 17 (1972).

20. W. Kutschera, R.B. Huber, C. Signorini and P. Blasi, Nucl. Phys. A210, 531 (1973).

21. B. Haas, P. Taras, J.C. Merdinger and R. Vaillancourt, Nucl. Phys. A238, 253 (1975).

22. L.P. Ekström, G.D. Jones, F. Kearns, T.P. Morrison, O.M. Mustaffa, D.N. Simister, H.G. Price, P.J. Twin, R. Wadsworth and N.J. Ward, J. Phys. G5, 803 (1979).

23. H. Hansen, P. Hornshoj and N. Rud, Nucl. Phys. A327, 193 (1979).

24. A.E. Macgregor and G. Brown, Nucl. Phys. 88, 385 (1966).

25. J.N. Mo, C.W. Lewis, M.F. Thomas and P.J. Twin, Nucl. Phys. A111, 657 (1968).

26. J.E. Robertshaw, S. Mecca, A. Sperduto and W.W. Buechner, Phys. Rev. 170, 1013 (1968).

27. P.A. Assimakopoulos, T. Becker, C. Moazed and D.M. Van Patter, Nucl. Phys. A180, 131 (1972).

28. S. Raman, R.L. Auble, W.T. Milner, J.B. Ball, F.K. McGowan, P.H. Stelson and R.L. Robinson, Nucl. Phys. A184, 138 (1972).

29. O. Hansen, T.A. Belote and W.E. Dorenbusch, Nucl. Phys. A118, 41 (1968).

30. W. Dehnhardt, O.C. Kistner, W. Kutschera and H.J. Sann, Phys. Rev. C7, 1471 (1973).

31. W. Kutschera, R.B. Hulser, C. Signorini and H. Morinaga, Phys. Rev. Lett. 33, 1108 (1974).

32. B.A. Brown, D.B. Fossan, J.M. McDonald and K.A. Snover, Phys. Rev. C9, 1033 (1974).

33. W. Bohne, H. Fuchs, K. Grabisch, D. Hilscher, V. Jhanke, H. Kluge, T.G. Masterson and H. Morgenstern, Nucl. Phys. A245, 107 (1975).

34. C. Fahlander, K. Johansson, E. Karlson, and G. Possnert, Nucl. Phys. A291, 241 (1977).

35. C.W. Towsley, D. Cline and R.N Horoshko, Nucl. Phys. A250, 381 (1975).

36. J.N. Ginnochio, Phys. Rev. 144, 952 (1966).

37. R.W. Zurmühle, D.A. Hutcheon and J.J. Weaver, Nucl. Phys. A180, 417 (1972).

38. W. Gullholmer and Z.P. Sawa, Nucl. Phys. A204, 561 (1973).

39. P. Engelstein, M. Forterre, N. Schulz and J.P. Vivien, Nucl. Phys. A230, 358 (1974).

40. J. Kasagi and H. Ohnuma, J. Phys. Soc. Jpn. 45, 1009 (1978); ibid 48, 351 (1980).

41. A. McNair, Phil. Mag. 69, 559 (1961).

42. F.K. McGown, R.H. Stelson, R.L. Robinson, W.T. Milner and J.L.C. Ford, Jr., in Proceedings of the Conference on Nuclear spin parity assignment, Gatlinburg, Tennessee, 1965 (Academic, New York 1966), p. 222.

43. R.R. Wilson, A.A. Bartlett, J.J. Kraushaar, J.D. McCullen and R.A. Ristinen, Phys. Rev. 125, 1655 (1962); S. Malmskog, Nucl. Phys. 49, 239 (1963); M.S. Freedman, F. Wagner, Jr., F.T. Porter and H.H. Bolotin, Phys. Rev. 146, 791 (1966).

44. E.C. Booth, B. Chasen and K.A. Wright, Nucl. Phys. 57, 403 (1964).

45. S. Ofer and A. Schwarzschild, Phys. Rev. Lett. 3, 384 (1969).

46. J.J. Simpson, J.A. Cookson, D. Eccleshall and M.J.L. Yates, Nucl. Phys. 62, 385 (1965).

47. D.M. Van Patter, N. Nath, S.M. Shafroth, S.S. Malik and M.A. Rothman, Phys. Rev. 128, 1246 (1962).

48. K. Matsuda, Nucl. Phys. 33, 536 (1962); K. Veje, C. Droste, O. Hansen and S. Holm, Nucl. Phys. 57, 451 (1964); H. Funsten, N.R. Robertson and E. Rost, Phys. Rev. 134, B117 (1964).

49. G. Kaye and J.C. Willmott, Nucl. Phys. 71, 561 (1965); C.F. Monahan, N. Lawley, C.W. Lewis, I.G. Main, M.F. Thomas and P.S. Twin, Nucl. Phys. A120, 460 (1968).

50. C.A. Whitten, Jr., Phys. Rev. 156, 1228 (1967).

51. R. Chapman, S. Hinds and A.E. Macgregor, Nucl. Phys. A119, 305 (1968); R.F. Casten, E.R. Flynn, O. Hansen and T.J. Mulligan, Phys. Rev. C4, 130 (1971).

52. W.P. Alford, R.A. Lindgren, D. Elmore and R.N. Boyd, Nucl. Phys. A243, 269 (1975).

53. A.A. Katsanos and J.R. Huizenga, Phys. Rev. 159, 931 (1967).

54. D.D. Armstrong and A.G. Blair, Phys. Rev. 140, B1226 (1965).

55. S.W. Sprague, R.G. Arns, B.J. Brunner, S.E. Caldwell and C.M. Rosza, Phys. Rev. C4, 2074 (1971).

56. F. Pellegrini, I. Filosofo, M.I. El Zaiki and I. Gabrielli, Phys. Rev. C8, 1547 (1973).

57. D.L. Watson and G. Brown, Nucl. Phys. A296, 1 (1978).

58. S. Fortier, E. Hourani, M.N. Rao and S. Gales, Nucl. Phys. A311, 324 (1978).

59. J. Meriwether, I. Gabrielli, D.L. Hendrie, J. Mahoney and B.G. Harvey, Phys. Rev. 146, 804 (1966).

60. M. Matoba, Nucl. Phys. A118, 207 (1968).

61. A. Berinde et al., Nucl. Phys. A284, 65 (1977).

62. A.R. Poletti, B.A. Brown, D.B. Fossan and E.K. Warburton, Phys. Rev. C10, 2329 (1974).

63. M.C. Lemaire, J.M. Loiseaux, M.C. Mermaz, A. Papineau and H. Faraggi, in Proceedings of the topcial Conference on the Structure of $1f_{7/2}$ Nuclei, Padova, 1971, edited by R.A. Ricci (Editrice Compositori, Bologna 1971), p. 201.

64. R.P. Yaffe and R.A. Meyer, Phys. Rev. C16, 1581 (1977).

65. A. de-Shalit, in Selected Topics in Nuclear Theory, edited by F. Janouch (IAEA, Vienna, 1963), p. 209.

66. I. Talmi and I. Unna, Ann. Rev. Nucl. Sci. 10, 353 (1960).

67. N. Auerbach, Phys. Lett. 24B, 260 (1967).

68. K. Lips and M.T. McEllistrem, Phys. Rev. C1, 1009 (1970).

69. M.L. Rustgi, R.P. Singh, B.B. Roy, R. Raj and C.C. Fu, Phys. Rev. C3, 2238 (1971).

70. B.B. Roy, R. Raj and M.L. Rustgi, Phys. Rev. C1, 207 (1970).

71. E. Osnes, in Proceedings of the Topical Conference on the Structure of $1f_{7/2}$ Nuclei, edited by R.A. Ricci (Editrice Compositori, Bologna, Italy, 1971), p. 79.

72. D.S. Chuu, C.S. Han, M.C. Wang and S.T. Hseih, J. Phys. G5, 59 (1979).

73. B. Haas et al., Phys. Rev. Lett. 40, 1313 (1978).

74. A. Yokoyama, T. Oda and H. Horie, Prog. Theor. Phys. 60, 427 (1978).

75. I.P. Johnstone, Phys. Rev. C17, 1428 (1978).

76. S.K. Sharma, Phys. Lett. 53B, 155 (1974).

77. H. Müther, K. Goeke, A. Faessler and K. Allart, Phys. Lett. 60B, 427 (1976).

78. D.P. Ahalpara, Phys. Rev. C22, 2619 (1980).

79. T.E. Ward, P.H. Pile and P.K. Kuroda, Nucl. Phys. A148, 225 (1970).

80. D.S. Andreyev, A.P. Grinberg, K.I. Erokhina and I.Kh. Lemberg, Nucl. Phys. 19, 400 (1960).

81. D.G. Alkhazov, A.P. Grinberg, K.I. Erokhina and I. Kh. Lemberg, Izv. Akad. Nauk SSSR (Ser. fiz.) 23, 223 (1959); Columbia tech. transl. 23, 215 (1960).

82. J.H. Bjerregaard, P.F. Dahl, O. Hansen and E. Sidenius, Nucl. Phys. 51, 641 (1964).

83. D.H. White, Phys. Rev. 131, 777 (1963).

84. G.A. Bartholomew and M.R. Gunye, Can. J. Phys. 43, 1128 (1965).

85. G. Brown, A. Denning and A.E. Macgregor, Nucl. Phys. A153, 145 (1970).

86. V.P. Bochin et al., Nucl. Phys. 51, 161 (1964).

87. D.C. Kocher and W. Haeberli, Nucl. Phys. A252, 381 (1975).

88. A.J. Elwyn and F.B. Shul, Phys. Rev. 111, (1958) 925.

89. A.M. Nathan, J.W. Olness, E.K. Warburton and J.B. McGrory, Phys. Rev. C17, 1008 (1978).

90. A.M. Nathan, D.E. Alburger, J.W. Olness and E.K. Warburton, Phys. Rev. C16, 1566 (1977).

91. J. Vervier, Nucl. Phys. 78, 497 (1966).

92. J.B. McGrory, Phys. Rev. 160, 915 (1967).

93. H. Horie and K. Ogawa, Nucl. Phys. A216, 407 (1973).

94. K.H. Bhatt, J.K. Parikh and J.B. McGrory, Nucl. Phys. A224, 301 (1974).

95. K. Ogawa, Phys. Rev. C15, 2209 (1977).

96. S. Saini and M.R. Gunye, Nucl. Phys. and Solid State Phys. (India) 21B, 84 (1978).

97. A. Dhar and K. Bhatt, Phys. Rev. C4, 1630 (1976).

TABLE I. Intrinsic states of even-A chromium isotopes included in the present calculations. The band quantum number K, energy E_K^{HF} and mass quadrupole moments $Q_K^{HF}(p)$ of protons and $Q_K^{HF}(n)$ of neutrons are tabulated for $^{48,50,52,54}Cr$.

Nucleus	K	E_K^{HF}(MeV)	$Q_K^{HF}(p)(fm^2)$	$Q_K^{HF}(n)(fm^2)$
^{48}Cr	0	-29.6	47.3	47.3
	0	-27.2	-30.4	-30.4
	4	-26.0	37.9	47.3
	4	-25.3	-25.6	-30.4
	2	-24.6	-23.3	-30.3
^{50}Cr	0	-38.1	41.6	40.8
	0	-36.1	-29.2	-24.6
	4	-35.8	32.9	40.8
	2	-35.3	-29.2	-21.9
	0	-34.8	41.5	18.6
	0	-34.7	24.0	40.6
	4	-34.5	-23.8	-24.6
	0	-34.4	-29.1	-19.3
	2*	-33.8	41.5	58.5
^{52}Cr	0	-44.7	34.0	9.9
	0	-44.6	-28.6	-10.2
	4	-43.5	-22.6	-10.2
	4	-43.4	26.3	9.9
	2	-43.3	15.6	9.9
	2	-43.2	-19.4	-10.1
	4*	-40.0	34.0	39.8

Table I (con't.)

Nucleus	K	E_K^{HF}(MeV)	$Q_K^{HF}(p)(fm^2)$	$Q_K^{HF}(n)(fm^2)$
^{54}Cr	0	-44.8	43.9	49.7
	0	-42.1	-29.2	-29.8
	4	-42.2	35.0	49.7
	2	-41.3	24.1	49.6
	4	-40.8	-24.2	-29.8
	0	-40.7	26.0	49.4
	2	-40.3	-21.6	-29.7

TABLE II. The electric quadrupole moment Q and magnetic dipole moment μ of the low-lying positive parity states in $^{48,50,52,54}Cr$. Effective charges employed in the present calculations are e_p=1.33e and e_n=0.64e.

Nucleus	J	Q(e fm^2) Expt.[a]	Calc.	SM[b]	$\mu(\mu_N)$ Expt.[c]	Calc.	SM[b]
	2		-27.1	0		1.04	1.08
^{48}Cr	4		-34.5	0		2.21	2.16
	6		-35.2	0		3.28	3.24
	2	-32±9	-23.4	-11.4	1.18±0.20	1.37	1.14
^{50}Cr	4		-26.9	- 9.1		2.90	3.69
	6		-20.6	8.5		4.50	4.31
	2	-14±8	- 4.6	- 5.8[d]		3.02	2.91
^{52}Cr	4		-15.5	0		5.99	5.82
	6		- 1.8	0		9.32	8.74
	2	-21±8	-27.6	- 0.7[d] -27.0[e]	1.12±0.20	1.48	1.44[e]
^{54}Cr	4		-33.8			3.16	
	6		-36.5			5.04	

a) Reference 35.

b) Reference 3. $(0f_{7/2})^n$ shell model calculations using effective operators with e_p=1.9e and e_n=0.9e; and g_p=1.456 μ_N and g_n=-0.377 μ_N

c) Reference 34.

Table II (con't.)

d) Reference 35. Configuration mixing shell model calculations using configurations of the type $(f_{7/2})^{12}+(f_{7/2})^{11}(p_{3/2}f_{5/2})^1$ for ^{52}Cr and $(f_{7/2})^{12}(p_{3/2})^2+(f_{7/2})^{11}(p_{3/2}f_{5/2})^3$ for ^{54}Cr and employing effective operators with e_p=1.5e, and e_n=1.0e.

e) Reference 93. Shell model calcualtions in the $\pi(f_{7/2})^4\nu(p_{3/2}, p_{1/2}f_{5/2})^2$ configuration space by employing effective operators with e_p=2.0e and e_n=1.0e; and $g_s(p)$ = 5.58 μ_N, $g_s(n)$=-3.82 μ_N.

TABLE III. The B(E2) and B(M1) values for γ-transitions in ^{48}Cr between positive parity states J_i and J_f. The subscript indicates the first excited states. The effective charges used are e_p=1.33e and e_n=0.64e.

		B(E2) e^2 fm^4			B(M1) μ_N^2	
J_i	J_f	Expt.	Calc	SM[a]	Calc	SM[a]
2	0	310.9±31.1[b]	200.1	152.1		
		207 ±27[c]				
4	2	248.7±62.2[b]	280.3	184.1		
6	4	>82.9[b]	290.2	186.8		
5	4		227.5	0	0.92	0
8	6	>41.4[b]	273.9	196.2		
7	5		71.4	60.1		
7	6		158.4	0	1.52	0
10	8		192.2	182.2		
9	7		85.2	33.5		
9	8		48.3	0	0.60	0
9	10		0.4	63.0	2.10	0
12	10		12.6	160.5		
11	9		1.3	62.6		
11	10		1.1	0	0.59	0
11	12		1.0	64.2	4.50	0
2_1	0		0.7	0		
2_1	2		39.1	198.6	0	0
2_1	4		1.4	0		
4_1	2		0.1	0		
4_1	4		2.2	156.4	0.43	0

Table III (con't.)

		B(E2) e^2 fm^4			B(M1) μ_N^2	
J_i	J_f	Expt.	Calc	SM[a]	Calc	SM[a]
4_1	6		0.2	0		
6_1	4		2.8	0		
6_1	8		0.4	0		
2_1	4_1		104.1	112.7		
6_1	4_1		76.3	79.9		

a) Reference 3. The shell model calculations are carried out in the $(f_{7/2})^8$ model space with e_p=1.9e and e_n=0.9e.

b) Reference 22.

c) Reference 20.

TABLE IV. The B(E2) and B(M1) values for γ transitions between the positive parity states in ^{50}Cr. Other details are same as in Table III.

		B(E2; $J_i \to J_f$) e^2 fm^4			B(M1; $J_i \to J_f$) μ_N^2		
J_i	J_f	Expt.[b]	Calc.	SM[a]	Expt.[d]	Calc.	SM[a]
2	0	223.2±21.9[c]	160.9	136.1			
4	2	156.5±19.7	221.3	176.1			
6	4	131.0±32.8	214.5	141.8			
8	6	>21.9	102.4	150.0			
10	8	>21.9	110.6	84.0			
12	10		94.8	73.6			
5	3		16.0	29.4			
5	4		191.4	0.3		0.78	0
5	6		134.0	69.1		0.61	0.24
7	5		70.1	47.7			
7	6		30.6	0.5		0.40	0.02
7	8		61.9	28.9		1.80	1.09
9	7		34.2	26.9			
9	8		8.5	1.2		0.0	0.0
9	10		0.1	0.6		1.20	0.77
11	9		63.6	83.0			
11	10		3.7	27.8	0.7>M1>0.2[b]	0.06	0.27
12	11		3.5	28.1	>1.1[b]	0.83	2.07
2_1	0	$8.5^{+3.2}_{-3.0}$[d]	3.4	9.9			
2_1	2	$1.2^{+5.2}_{-1.2}$[d]	36.2	39.3	$0.42^{+0.07}_{-0.05}$	0.15	1.22
2_1	4		0.1	6.6			

Table IV (con't.)

		B(E2; $J_i \to J_f$) e^2 fm^4			B(M1; $J_i \to J_f$) μ_N^2		
J_i	J_f	Expt.[b]	Calc.	SM[a]	Expt.[d]	Calc.	SM[a]
4_1	2		3.2	0.7			
4_1	4	<210[d]	20.5	93.2	$0.14^{+0.05}_{-0.03}$	0.06	0.14
4_1	6		0.5	1.0			
4_1	2_1		6.3	25.6			

a) Reference 3. $(0f_{7/2})^n$ shell model calculations employing effective operators with e_p=1.9e and e_n=0.9e.

b) Reference 31.

c) Weighted average of References 28. 30, 31, 35, 37 and 38.

d) Reference 27.

TABLE V. The B(E2) and B(M1) values for transitions between the low-lying positive parity states belonging to the ground band (i.e. the states having dominant $f_{7/2}^n$ character) in ^{52}Cr. Other details are the same as in Table III.

		B(E2; $J_i \to J_f$) e^2 fm^4			B(M1; $J_i \to J_f$)$\mu_N^2 \times 10^{-3}$		
J_i	J_f	Expt.[a]	Calc.	SM[b]	Expt.[a]	Calc.	SM[f]
2	0	133±6[c]	55.7	105.5			
4	2	83±17[d]	90.6	116.6			
6	4	59.1±2.0	70.5	97.4			
5	4	<30[e] 0.8-17.7	63.8	0	<3.2[e] 2.1-8.0	4.0	0.3
5	6	<2305[e]	82.3	80.1	<39[e] 5.7-29.3	24.0	3.7
8	6	75^{+27}_{-18}	21.0	75.4			
2_1	0	≤ 0.2[g]	9.0	0			
2_1	2	162±32	104.8	106.6	$0.66^{+0.71}_{-0.29}$	4.0	3.3
2_1	4		4.9	0			
4_1	2	70^{+34}_{-18}	5.1	0			
4_1	4	92^{+37}_{-24}[e]	45.4	112.0	20^{+23}_{-13}	13.0	2.4
6	4_1	33.0±5.6	6.8	0			
2_1	4_1		42.8	51.7			

a) Reference 13.

b) Reference 3. $(f_{7/2})^n$ shell model calculations using effective operators with e_p=1.9e, e_n=0.9e

c) Weighted mean of the B(E2) values of Refs. 38. 40, 42, 55 and 35.

Table V (con't.)

d) Reference 32.

e) Reference 55.

f) Reference 13. These shell model calculations are carried out in the $f_{7/2}^n + f_{7/2}^{n-1}(p_{3/2}f_{5/2}p_{1/2})^1$ configuration space using e_p=1.6e and e_n=0.6e

g) References 35, 43 and 51.

TABLE VI. The transition strengths for the γ transitions between the members of the $K^{\pi} = 4^{+}$ collective band in ^{52}Cr. Other details are same as in Table III.

J_i	J_f	B(E2; $J_i \to J_f$) (e^2 fm^4) Expt.[a]	Calc.	SM[a]	B(M1; $J_i \to J_f$) (μ_N^2) Expt.[a]	Calc.	SM[a]
5	4		201.0		100^{+70}_{-30}	162	98.6
6	5	66^{+223}_{-56}	202.7	39.0	110^{+190}_{-80}	2400	1317
6	4	<51	39.1	59.9			
7	6	640^{+2000}_{-450}	168.9	76.2	1100^{+1800}_{-500}	2900	5098
7	5	130^{+260}_{-70}	70.7	65.0			
8	7	34^{+115}_{-32}	134.2	0.0	480^{+280}_{-180}	2800	900
8	6	<117	90.1	49.4			
9	8	100^{+230}_{-80}	101.7	54.6	140^{+100}_{-50}	2090	54.7
9	7	<340	98.3	64.6			
10	9		76.3			2090	1190.8
10	8		107.1				
11	10		56.4			2760	191.3
11	9		108.9				
12	11		48.4			1930	
12	10		99.8				

a) Reference 13.

TABLE VII. The B(E2) and B(M1) values for the transitions between the positive parity states in ^{54}Cr. Other details are the same as in Table III.

J_i	J_f	B(E2; $J_i \to J_f$)(e^2fm^4) Expt.[a]	Calc.	SM[a]	B(M1;$J_i \to J_f$)(μ_N^2) Calc.
2	0	168±6[b]	194.1	204.9	
4	2	303±84	268.3	255.8	
6	4	218±61	267.6	224.3	
5	4		226.1		0.59
5	6		222.3		0.62
7	6		134.4		1.03
8	6	145.4±24.3	238.3	232.8	
9	7		103.1		
9	8		13.6		
10	8	> 145.4	173.6	172.2	
12	10		116.9		
11	9		86.8		
11	10		15.6		0.08
11	12		16.2		2.45
2_1	0		3.3		
2_1	2		20.0		0.01
4_1	2		0.1		
4_1	4		1.6		
4_1	6		0.3		
6_1	4		1.9		

Table VII (con't.)

J_i	J_f	B(E2; $J_i \rightarrow J_f$)(e^2fm^4) Expt.[a]	Calc.	B(M1;$J_i \rightarrow J_f$)(μ_N^2) SM[a]	Calc.
8	6_1		23.6		
4_1	2_1		16.0		
6_1	4_1		54.3		

a) Reference 89. Shell model calculations in the $(0f_{7/2})^4$ $(1p_{3/2}, 1p_{1/2}, 0f_{5/2})^2$ configuration space using effective operators with e_p=2.0e and e_n=1.0.

b) Weighted average of the B(E2) values of Refs. 35, 42, 80 and 81.

Figure Captions

FIG. 1. Comparison of theoretical and experimental energy spectra for positive parity states in ^{48}Cr. The numbers on the right of the levels indicate J values.

FIG. 2. The schematic Nilsson diagram for the ground and excited intrinsic states of ^{50}Cr with prolate deformation. The excited intrinsic state is obtained by 1p-1h elementary neutron excitation. The ground and the exicted intrinsic states correspond to the filling of the deformed orbitals at different deformations δ_a and δ_b respectively.

FIG. 3. The theoretical and experimental energy spectra of positive parity states in ^{50}Cr. The right hand part of the spectrum shows the collective band of states projected from $K^\pi = 2^+$ deformed band. The numbers on the right of the levels indicate J values.

FIG. 4. The theoretical and experimental energy spectra of positive parity states in ^{52}Cr. The left hand part of the spectrum exhibits levels belonging to the 'ground state band' with a predominant $(0f_{7/2})^n$ component, where as the right-hand part of the spectrum shows the collective band of states belonging to the deformed $K^\pi = 4^+$ band.

FIG. 5. The calculated and epxerimental energy spectra of positive parity states in ^{54}Cr. Other detaila are same as in figure 1.

FIG. 1

MSUX-81-051